

# Coupling between two collinear air-core Bragg fibers

Maksim Skorobogatiy

*Genie Physique, Ecole Polytechnique de Montreal, C.P. 6079, succ. Centre-Ville Montreal, Quebec H3C3A7, Canada*

Kunimasa Saitoh and Masanori Koshiba

*Division of Media and Network Technologies, Hokkaido University, Sapporo 060-0814, Japan*

Received January 16, 2004; revised manuscript received July 20, 2004; accepted July 31, 2004

We characterize coupling between two identical collinear hollow-core Bragg fibers, assuming a  $TE_{01}$  launching condition. Using a multipole method and a finite-element method, we have investigated the dependence of the beat length between supermodes of the coupled fibers and supermode radiation losses as a function of the interfiber separation, the fiber core radius, and the index of the cladding. We established that coupling is maximal when the fibers are touching each other and decreases dramatically during the first hundreds of nanometers of separation. However, residual coupling with the strength proportional to the fiber radiation loss decreased over a long range as an inverse square root of the interfiber separation and exhibited periodic variation with interfiber separation. Finally, we considered coupling between the  $TE_{01}$  modes with a view to designing a directional coupler. We found that for fibers with large enough core radii one can identify broad frequency ranges in which the intermodal coupling strength exceeds supermode radiation losses by 1 order of magnitude, thus opening the possibility of building a directional coupler. We attribute such unusually strong intermode coupling both to the resonant effects in the intermirror cavity and to proximity interaction between the leaky modes localized in the mirror. © 2004 Optical Society of America

*OCIS codes:* 060.2310, 060.2400, 060.2280.

## 1. INTRODUCTION

Recently, hollow-core photonic bandgap (PBG) microstructured and Bragg fibers were experimentally demonstrated to exhibit guidance and low transmission loss at 1.55,<sup>1</sup> 3.0, and 10.6  $\mu\text{m}$ ,<sup>2</sup> promising a considerable effect on long-haul and high-power guidance applications almost anywhere in the IR. Hollow PBG fibers are able to guide light through the hollow (gaseous) core, exhibiting low material loss and nonlinearity and achieving radiation confinement by reflection from the surrounding high-quality dielectric multilayer mirror. Development of such fibers motivated interest in the design of directional couplers based on PBG fibers to provide a uniform guiding-switching fabric in which the same type of fiber is used to guide and to manipulate light.

Because of the wide availability of microstructured PBG fibers, most of the recent experimental and theoretical work has concentrated on the design of directional couplers based on such fibers.<sup>3-7</sup> In particular, in the preform stage silica rods are arranged to form two closely spaced silica or air cores separated by several air-silica layers, all surrounded by a hexagonal lattice of silica rods. When a preform is drawn, the resultant microstructured fiber exhibits two closely spaced identical cores surrounded by a photonic crystal reflector. Coupling between such cores is characterized by a finite-element or finite-difference method with integrated absorbing boundary conditions.<sup>8-11</sup>

In this paper we consider, for the first time to our

knowledge, coupling between PBG fibers of another type: hollow Bragg fibers. Our main interest is to characterize the coupling strength between collinear PBG Bragg fibers and the propagation losses of the lowest-loss “telecommunication quality”<sup>12</sup>  $TE_{01}$ -like supermodes. The issue of interfiber modal coupling can be of importance when several hollow photonic crystal fibers are placed in near proximity because of the long radiation-driven interaction range between such fibers that we establish in this paper. We also address the possibility of building Bragg-fiber-based directional couplers for  $TE_{01}$  modes. Unlike for PBG microstructured fibers, the current process of Bragg fiber fabrication does not allow the cores of two Bragg fibers to be placed arbitrarily close, while keeping a common PBG reflector on the outside of both cores. We show that enhanced resonant coupling is still possible even with standard Bragg fibers by tuning of the separation between them to specific values with Bragg fiber mirrors of adjacent fibers, creating an open resonant cavity.

The outline of our paper is as follows: We start by justifying most of the coupling properties between collinear PBG Bragg fibers based on the analogy with one-dimensional Bragg gratings with defects. We then characterize the interfiber coupling as a function of core separation and index of the cladding, using multipole and finite-element methods. Finally, we discuss the possibility of building a directional coupler based on the resonant interaction between the fibers. In Appendix A we comment on some modifications to the original multipole method<sup>13</sup> that are necessary to treat coupled Bragg fibers.

## 2. ANALOGY TO A ONE-DIMENSIONAL BRAGG GRATING WITH DEFECTS

We consider two collinear hollow PBG Bragg fibers of core radius  $R_c$ , outer mirror radius  $R_o$ , and intermirror separation  $d$ . In Fig. 1 we present schematics of the system together with a dielectric profile along the line passing through the fiber centers. We assume that the PBG mirror is made from two dielectrics with refractive indices  $n_h > n_l > n_c$ , where  $n_c$  is a core index (for hollow fibers  $n_c = 1$ ) and the corresponding mirror layer thicknesses  $d_h$  and  $d_l$  are chosen to form a quarter-wave stack for the grazing angles of incidence.<sup>12</sup> Thus, denoting by  $\lambda$  the center wavelength of the PBG yields  $d_h[n_h^2 - n_c^2]^{1/2} = d_l[n_l^2 - n_c^2]^{1/2} = \lambda/4$ . Cladding index  $n_{\text{clad}}$  can be chosen at will.

Inspection of Fig. 1 shows a dielectric profile along the fiber center line that resembles a one-dimensional Bragg grating made from the fiber reflector mirrors and a central defect of size  $d$  corresponding to the intermirror cavity. The quarter-wave thickness of each mirror layer ensures the largest bandgap (stop band) of the reflector Bragg grating, so radiation incoming from the hollow core onto the containing mirror will be maximally reflected. However, when the optical length of the central defect in the Bragg grating is  $\lambda\nu/2$ ,  $\nu \in (0, 1, \dots)$ , it is known that transmission through such a grating will exhibit a narrow maximum at  $\lambda$ , although transmission everywhere else in the Bragg grating stop band will still be strongly suppressed. When there are two identical Bragg fibers, the first resonance happens when the fibers are touching ( $d = 0$ ), as the two outside high-index layers of the fiber mirrors create a  $\lambda/2$  defect (Fig. 1). Introducing free-space wave number  $k = 2\pi/\lambda$ , modal propagation constant  $\beta$ , and a transverse modal wave number in the defect layer of refractive index  $n$  and thickness  $d$  as  $k_n^t = [(kn)^2 - \beta^2]^{1/2}$ , we rewrite the resonant condition for a half-wavelength defect as  $dk_n^t = \pi\nu$ . Thus, anytime intermirror separation  $d$  approaches its resonant value we expect an increase in the interfiber coupling owing to enhanced radiation leakage from one core to another me-

diated by the resonant intermirror cavity. The spectral width and the maximum of an enhanced coupling peak will be strong functions of the intermirror cavity  $Q$  factor. Because of the cylindrical shape of the fiber Bragg reflectors, the intermirror cavity  $Q$  factor is ultimately limited by the fiber's finite curvature,  $\sim R_o^{-1}$ . Finally, to increase the spectral width of a coupling peak one can adopt a standard solution from the theory of flattened passband filters<sup>14</sup> in which the structure of the Bragg reflector is modified to present a sequence of several low-quality  $\lambda/4$  stacks coupled together by  $\lambda/2$  defects, exhibiting a designable spectral width steplike transmission response.

We now address the effect of cladding index  $n_{\text{clad}}$  on the PBG Bragg fiber coupling. It was established in Ref. 12 that low-loss modes in PBG Bragg fibers have their propagation constants situated close to the core material's light line, particularly for the  $\text{TE}_{01}$  mode,  $1 - \beta/(kn_c) \sim (\lambda/R_c)^2$ . Typical values of the core radii for a long-haul PBG Bragg fiber<sup>12</sup> are  $R_c \sim 10\text{--}15\lambda$ . Thus in the core material  $k_{n_c}^t = [(kn_c)^2 - \beta^2]^{1/2} \sim R_c^{-1}$ , whereas in the material with  $n > n_c$ ,  $k_n^t \approx k[n^2 - n_c^2]^{1/2}$ . Thus if cladding index is the same as the core index,  $n_{\text{clad}} = n_c$ , one expects a resonant increase in the coupling between PBG Bragg fibers at  $d = \pi\nu/(k_{n_c}) \sim \nu R_c$ , whereas, if  $n_{\text{clad}} > n_c$ , then  $d \approx \lambda\nu/[2(n_{\text{clad}}^2 - n_c^2)^{1/2}]$ , where in both cases  $\nu \in (0, 1, \dots)$ .

Finally, as distance  $L = 2R_o + d$  between the fiber centers increases, the intensities of the radiated fields from the core of one fiber at the position of the second fiber will decrease with distance as  $E \sim (\text{Im}(\beta)/L)^{1/2}$ , where  $\text{Im}(\beta)$  is proportional to the modal radiation loss (from the energy-conservation argument). Classic consideration of interfiber coupling between similar modes suggests that the coupling strength is proportional to the overlap of the fields of one fiber in the mirror region of another fiber, leading to the dependence of the PBG Bragg fiber coupling strength according to  $\text{Im}(\beta)/\sqrt{L}$  with the modal loss and interfiber separation.

## 3. DIRECTIONAL COUPLING AS A FUNCTION OF INTERMIRROR SEPARATION

We first analyze the coupling between the lowest-loss telecommunication quality  $\text{TE}_{01}$  modes of the two collinear PBG Bragg fibers by employing the modified multipole method<sup>15</sup> outlined in Appendix A. In a stand-alone fiber,  $\text{TE}_{01}$  is a singlet, with zero electric-field components along the direction of propagation and the radial direction<sup>12</sup> (the electric-field vector is circling parallel to the dielectric interfaces). When a second identical fiber is introduced, the rotational symmetry of a single fiber is broken and interaction between the  $\text{TE}_{01}$  modes of the Bragg fibers leads to the appearance of two supermodes with propagation constants  $\beta^-$  and  $\beta^+$  close to  $\beta$ . The remaining symmetry of the system is described by the  $C_{2v}$  group, which includes reflections in the  $(XZ)$  and  $(YZ)$  planes and inversion with respect to system symmetry center  $O$  (see Fig. 1). Symmetry considerations result in the following symmetries of the transverse electric-field components of the supermodes: supermode<sup>-</sup>,  $E_x(x, -y) = -E_x(x, y)$ ,  $E_y(x, -y) = E_y(x, y)$ ,  $E_x(-x, y) = E_x(x, y)$ ,  $E_y(-x, y) = -E_y(x, y)$ ; supermode<sup>+</sup>,  $E_x(x, -y) = -E_x(x, y)$ ,  $E_y(x, -y) = E_y(x, y)$ ,

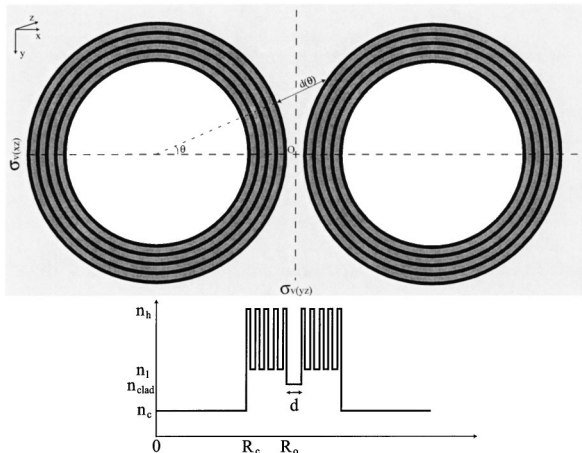


Fig. 1. Schematics of the two identical collinear hollow Bragg fibers separated by intermirror distance  $d$ . The Dielectric profile along the interfiber center line resembles a one-dimensional Bragg grating with a central defect corresponding to the intermirror cavity.

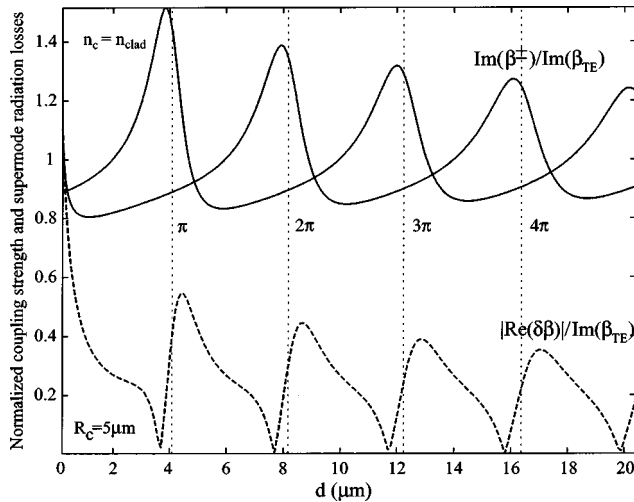


Fig. 2. Normalized coupling strength  $|\text{Re}(\delta\beta)|/\text{Im}(\beta_{\text{TE}})$  and supermode radiation losses  $\text{Im}(\beta^+)/\text{Im}(\beta_{\text{TE}})$  and  $\text{Im}(\beta^-)/\text{Im}(\beta_{\text{TE}})$  in a system of two collinear hollow Bragg fibers as a function of intermirror separation  $d$ . The cladding index is the same as the core index:  $n_c = n_{\text{clad}}$ . All the curves are normalized by the radiation losses of the  $\text{TE}_{01}$  mode of a stand-alone hollow Bragg fiber.

$E_x(-x, y) = -E_x(x, y)$ ,  $E_y(-x, y) = E_y(x, y)$ . Thus, at system symmetry center  $O$ , supermode<sup>+</sup> will have a local maximum of the electric field, whereas supermode<sup>-</sup> will have a node.

We first quantify the coupling strength between fibers and radiation losses of the supermodes as a function of intermirror separation  $d$  when  $n_c = n_{\text{clad}}$ . We characterize the interfiber coupling strength by the difference in the real parts of supermode propagation constants  $\delta\beta = |\beta^+ - \beta^-|$ , whereas modal radiation losses are defined by the imaginary parts of their propagation constants. The Bragg fiber under study has seven mirror layers (starting and ending with a high-index layer),  $n_c = 1$ ,  $n_h = 2.8$ ,  $n_l = 1.5$ ,  $n_{\text{clad}} = n_c = 1$ , and  $R_c = 5 \mu\text{m}$ ; the operating wavelength is  $1.55 \mu\text{m}$ . In Fig. 2 the normalized coupling strength and radiation losses of supermodes are presented. The normalization factor is the radiation loss of a  $\text{TE}_{01}$  mode, which for this fiber is 11.2 dB/m. Such a normalization choice allows us to largely decouple the structure of the reflector from other geometrical variables such as interfiber separation. One observes that coupling strength exhibits a periodic variation as the separation between fibers increases. Locations of the maxima in coupling strength match well the predicted half-wave condition for optical defect length  $d = \pi\nu/(k_{n_c}) \sim \nu R_c$  (marked by the vertical dotted lines in Fig. 2). Locations of the maxima in supermode losses are also close to the half-wave separation between fiber mirrors, suggesting that the increase in loss is due to field leakage out of the open intermirror cavity, where at resonance the field intensity is enhanced. From Fig. 2 one also observes a very slow decrease in coupling with interfiber separation. By analyzing the values of the coupling maxima as a function of distance up to  $d = 100 \mu\text{m}$ , one can observe a clear  $|\delta\beta| \sim (2R_o + d)^{-0.5}$  dependence.

As we argued in Section 2, when  $n_c = n_{\text{clad}}$  the position of the maxima of modal coupling scales proportionally to core radius  $R_c$ . In Fig. 3 we verify this scaling by plot-

ting normalized coupling and supermode radiation losses as a function of the interfiber separation for three Bragg fibers that have different core radii and the same dielectric profile as previously. The predicted scaling is clearly observable. In comparing the values of the modal coupling at the first maxima, one observes that the coupling slowly increases as the fiber core radius increases. Looking at the region of small intermirror separations  $0.2 \mu\text{m} < d < 1 \mu\text{m}$  (left-hand part of Fig. 3), one observes a substantial increase in the coupling strength that considerably surpasses the supermode radiation losses when the distance between mirrors is decreased. Moreover, for the same intermirror separation  $d$ , the coupling strength increases with an increase in the fiber core radius, signifying that the quality of the intermirror cavity resonator increases as  $R_c$  increases.

Overall, from Figs. 2 and 3, one observes that coupling between Bragg fibers remains comparable to the supermode radiation losses even at very large separations, whereas in the region of almost touching fibers  $d < 1 \mu\text{m}$  the coupling strength considerably exceeds supermode radiation losses. Thus, supermode beat length  $\pi/|\delta\beta|$  (the characteristic length of the fiber link after which a considerable amount of power in one fiber gets transferred into another fiber) remains comparable with supermode decay length  $1/\text{Im}(\beta^+)$  even for large interfiber separations  $d \sim 100 \mu\text{m}$ . Hence, extra care should be taken to absorb the radiation fields of the leaky modes when one is dealing with closely spaced Bragg fibers.

Next, we investigate the coupling strength between fibers and supermode radiation losses as a function of intermirror separation  $d$  when  $n_{\text{clad}} > n_c$ . The Bragg fibers under study have the same dielectric profile and operating wavelength as previously, except for the value of the cladding index,  $n_{\text{clad}} = 1.3$ . In Fig. 4 we present the normalized coupling strength and supermode radiation losses for three Bragg fibers, of core radii  $R_c = 5 \mu\text{m}$ ,  $R_c = 10 \mu\text{m}$ , and  $R_c = 20 \mu\text{m}$ , as functions of the intermirror separation about their second maxima.

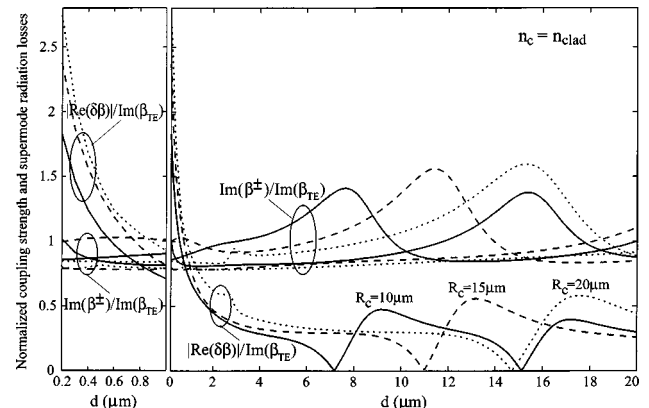


Fig. 3. Normalized coupling strength and supermode radiation losses of coupled hollow Bragg fibers as a function of intermirror fiber separation  $d$ . The cladding index is the same as the core index:  $n_c = n_{\text{clad}}$ . Bragg fibers of three core radii are studied: solid curves,  $R_c = 10 \mu\text{m}$ ; dashed curves,  $R_c = 15 \mu\text{m}$ ; dotted curves,  $R_c = 20 \mu\text{m}$ . At the left is a blowup of the region where fibers nearly touch ( $0.2 \mu\text{m} < d < 1 \mu\text{m}$ ), showing a dramatic increase in the fiber coupling compared to the almost constant radiation losses of the supermodes.

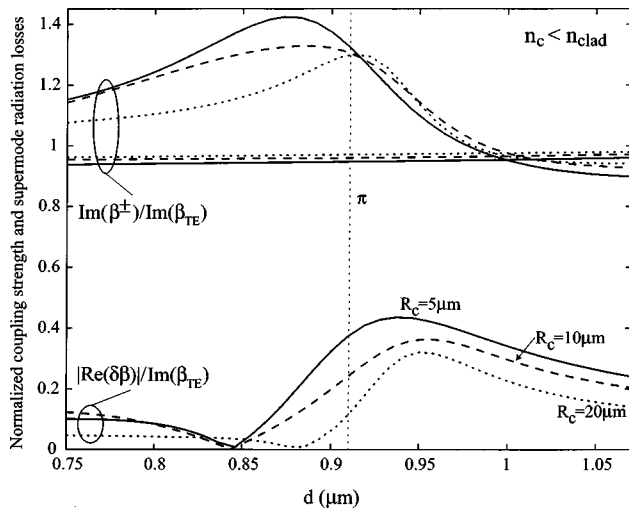


Fig. 4. Normalized coupling strength and supermode radiation losses of coupled hollow Bragg fibers as a function of intermirror fiber separation  $d$  near second resonance. The cladding index is larger than the core index:  $n_{\text{clad}} = 1.3$ ,  $n_c = 1$ . Bragg fibers of three core radii are shown: solid curves,  $R_c = 5 \mu\text{m}$ ; dashed curves,  $R_c = 10 \mu\text{m}$ ; dotted curves,  $R_c = 20 \mu\text{m}$ . The maximum of the coupling strength slowly decreases as the fiber core radius increases.

Inspecting Fig. 4 reveals that, independently of the fiber core radius, the locations of the second maxima  $\nu = 1$  in the coupling strength match well the predicted maxima based on the half-wave condition for optical defect length  $d = \lambda \nu / [2(n_{\text{clad}}^2 - n_c^2)^{1/2}]$  (marked by the dotted curves in Fig. 4). On comparing the values of the fiber coupling at the first maxima, one observes that the coupling slowly decreases as the fiber core radius increases.

The differences in behavior of the interfiber coupling strength with the change of fiber core radius  $R_c$  for  $n_c = n_{\text{clad}}$  and  $n_{\text{clad}} > n_c$  can be rationalized as follows: Resonant phenomena in the intermirror cavity come from coherent addition of the multiply reflected radial waves that are originally radiated from the fiber core. The phase difference that a radial wave experiences in traversing from the first mirror to the second depends strongly on the intermirror separation  $d(\theta)$ . In turn, intermirror separation depends on angle  $\theta$  (Fig. 1) at which the wave escapes the core. For small angles and  $d \ll R_o$ ,  $d(\theta) \approx d(0) + R_o \theta^2$ . The phase shift that the radial wave experiences after one trip is  $\phi(\theta) = d(\theta)k_n^t$ , where  $k_n^t$  is a transverse wave number. Thus, waves traveling at different angles will have somewhat different phases, and, at some critical  $\theta_c$ , phase difference  $\phi(\theta_c) - \phi(0) = \pi$  will lead to destructive interference of waves in the intermirror cavity. The larger  $\theta_c$  is, the higher the quality of the resonator will be. When  $n_c = n_{\text{clad}}$ ,  $\phi(\theta) - \phi(0) = R_o \theta^2 k_{n_c}^t$ , and as  $k_{n_c}^t \sim R_c^{-1}$  and  $R_c \sim R_o$  we arrive at  $\theta_c \sim 1$ , which is independent of the core radius. In contrast, when  $n_{\text{clad}} > n_c$ ,  $\phi(\theta) - \phi(0) = R_o \theta^2 k_n^t$ , and as  $k_n^t \approx \omega(n^2 - n_c^2)^{1/2}$ , then  $\theta_c \sim \sqrt{\lambda/R_c}$ , thus slowly decreasing as the core radius increases. Hence when  $n_{\text{clad}} > n_c$  the quality of the resonator decreases when the core radius is increased, whereas the opposite is true for  $n_{\text{clad}} = n_c$ .

Finally, we have also observed that the multipole method,<sup>13</sup> although it performs efficiently at intermirror

separations  $d/R_o > 0.1$ , exhibits slow convergence at smaller separations, and at  $d/R_o < 0.01$  convergence becomes problematic. To further study touching fibers we resort to a finite-element mode solver with absorbing boundary conditions.

#### 4. DIRECTIONAL COUPLING AS A FUNCTION OF WAVELENGTH

In this section we study the feasibility of designing a directional coupler based on two touching hollow Bragg fibers studied by the finite-element mode solver.<sup>8</sup> In what follows, we assume the same structure of the two Bragg fibers as before; now the fibers are touching along their length ( $d = 0$  in Fig. 1). The fibers are designed for 1.55- $\mu\text{m}$  operation wavelength with the index of the cladding matched with that of a core,  $n_{\text{clad}} = n_c = 1$ . First we characterize the coupling strength between fibers and radiation losses of the supermodes as a function of fiber core radii  $R_c$  at a fixed frequency,  $\lambda = 1.45 \mu\text{m}$ . Because of the cylindrical shape of the fiber Bragg reflectors, the intermirror cavity  $Q$  factor is limited by the mirror's finite curvature, with  $Q$  and, thus, interfiber coupling increasing for larger core radii. In Fig. 5 the normalized coupling strength and radiation losses of supermodes are presented. The normalization factor for each curve is a corresponding radiation loss of the  $\text{TE}_{01}$  mode of a stand-alone fiber. One observes that with increasing core radius the coupling strength exhibits a tendency toward a gradual increase relative to the radiation losses of the supermodes. For core radii larger than 10  $\mu\text{m}$  the ratio of the coupling strength to the supermode radiation loss approaches a factor of 10, in principle permitting a directional coupler to be built. Resonant features correspond to the points of accidental degeneracy of  $\text{TE}_{01}$  with higher-order modes.

In Fig. 6 we plot normalized coupling strength and supermode radiation losses as a function of wavelength  $\lambda$  for  $R_c = 15 \mu\text{m}$  and three interfiber separations:  $d = 0$ ,  $d$

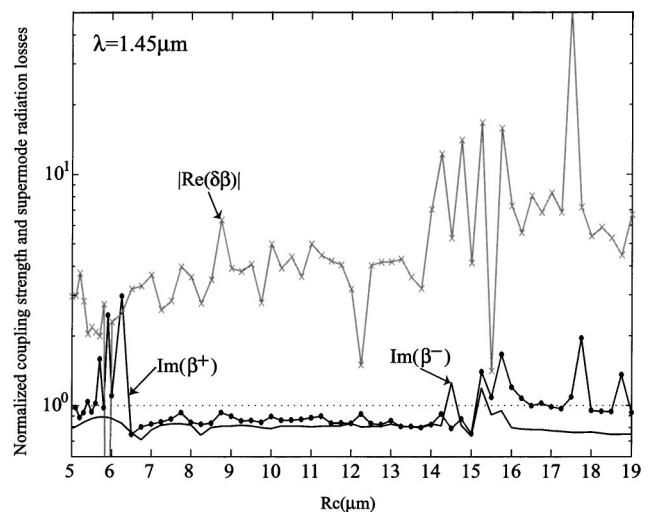


Fig. 5. Normalized coupling strength and supermode radiation losses as a function of fiber core radii  $R_c$  at  $\lambda = 1.45 \mu\text{m}$ . With increasing core radius one observes a tendency for a gradual increase of the coupling strength relative to the highest radiation loss of the supermodes.

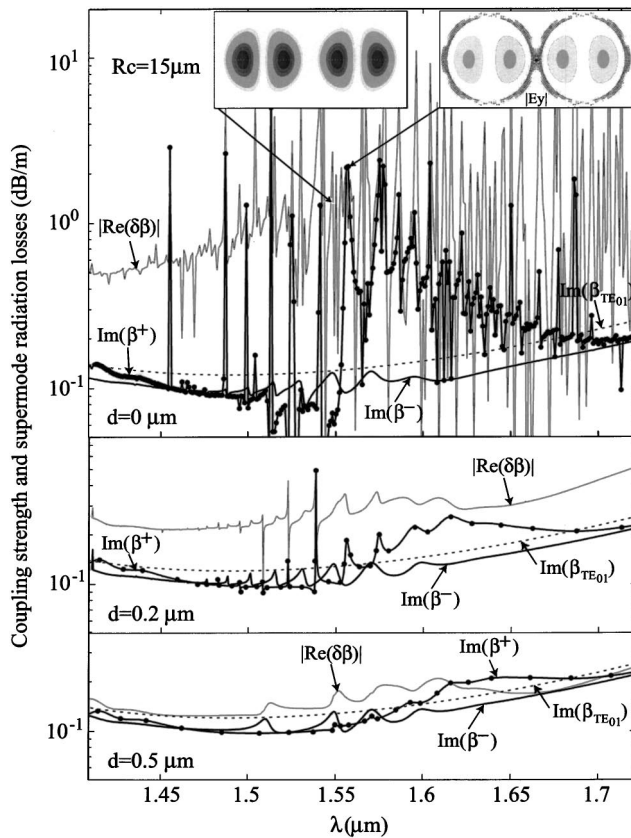


Fig. 6. Normalized coupling strength and supermode radiation losses as functions of wave-length  $\lambda$  for  $R_c = 15 \mu\text{m}$  and inter-fiber separations  $d = 0, 0.2, 0.5 \mu\text{m}$ . Dotted curve,  $\text{Im}(\beta_{\text{TE}_{01}})$ ; solid curve below dotted curve,  $\text{Im}(\beta^-)$ ; solid curve with filled circles,  $\text{Im}(\beta^+)$ ; solid curve above dotted curve,  $|\text{Re}(\delta\beta)|$ .

$= 0.2$ , and  $d = 0.5 \mu\text{m}$ . For  $d = 0.5 \mu\text{m}$  the coupling strength is weak and is of the order of the supermode radiation losses, changing smoothly as a function of frequency. As the inter-fiber separation decreases, the coupling strength exhibits a rapid increase across a broad frequency range, together with the appearance of many sharp resonances ( $d = 0.2 \mu\text{m}$  in Fig. 6). When fibers are touching,  $d = 0 \mu\text{m}$  the coupling strength strongly dominates supermode radiation losses in a broad frequency range. For  $1.4 \mu\text{m} < \lambda < 1.55 \mu\text{m}$ , for example, the ratio of coupling strength to the supermode radiation losses reaches a factor of 10. For a corresponding planar system of grating-defect-grating with a dielectric profile of Fig. 1 the resonance peak is, however, only several nanometers wide, in contradiction to the very broad resonant features of Fig. 6. Thus a simple picture of enhanced inter-fiber coupling has to be modified. As the spectral width of the enhanced coupling peak depends strongly on the intermirror cavity  $Q$  factor, we believe that the broad resonant features in Fig. 6 can be explained by the low  $Q$  factor of the resonant intermirror cavity, which is due to finite curvature of the fiber. As our mode solver was limited to core radii less than  $20 \mu\text{m}$ , we were not able to investigate further the narrowing of the resonance for larger radii. Another prominent feature of Fig. 6 is the presence of sharp and broad regions of increase in the supermode losses. Because of the multi-

mode nature of hollow Bragg fibers, the lowest-loss  $\text{TE}_{01}$  mode exhibits multiple points of accidental degeneracy with higher-loss modes. At such degeneracy points a  $\text{TE}_{01}$ -like supermode exhibits a sharp loss increase by picking up some of the higher-order mode loss. In general, we find that broad frequency regions of increase in the supermode losses are due to interaction with low-angular-momentum modes. For example, by inspecting the band diagram of a stand-alone fiber we found that in the region  $1.55 \mu\text{m} < \lambda < 1.65 \mu\text{m}$  an  $m = 2$  mode crosses the  $\text{TE}_{01}$  mode twice, staying almost degenerate with it in the whole interval. In Fig. 6 ( $d = 0 \mu\text{m}$ ) this broad modal interaction region is characterized by an increase in the supermode loss. We further verified our assumption by modifying the location of the modal degeneracy region by adding more layers to the reflector; we observed a consistent shift of a broad resonance. By inspecting the modal fields about the sharp resonances (Fig. 6, insets;  $d = 0 \mu\text{m}$ ), however we concluded that such resonances correspond to the points of degeneracy of a  $\text{TE}_{01}$  mode with the high-angular-momentum mirror modes. At resonance, a hybrid mode has its intensity maximum in the intermirror cavity defect and the outermost minor layers, whereas the fields in the hollow fiber cores are reduced. We have verified that in a stand-alone fiber there is a large number of high-angular-momentum  $m > 6$  leaky modes with propagation constants close to the air line and fields concentrated mostly in the outermost layers of the fiber reflector. In a region just outside the fiber such modes exhibit fast decay in the cladding. Thus, sharp resonances that are due to interaction with such modes disappear quickly with increases in the inter-fiber separation, as is clearly observable from Fig. 6 [ $d = 0, 0.2, 0.5 \mu\text{m}$ ].

## 5. DISCUSSION

To summarize, we have found that, unlike in silica fibers in which the modal tail decays exponentially into the cladding, the radiation field from a hollow PBG Bragg fiber decays slowly in the cladding as an inverse of the square root of the inter-fiber separation, exhibiting periodic oscillation. Moreover, the beat length between supermodes [ $\pi/\text{Re}(\beta^+ - \beta^-)$ ] remains of the order of supermode decay length  $l/\text{Im}(\beta^\pm)$  even for very large inter-fiber separations of  $\sim 100 \mu\text{m}$ . When two straight pieces of PBG Bragg fiber were spaced less than  $1 \mu\text{m}$  from each other we observed a dramatic increase in modal coupling without a substantial increase in supermode losses. We demonstrated that, for two touching PBG Bragg fibers of substantially large core radius, the frequency regions can be identified in which a large increase in the modal coupling is observed without a substantial increase in the supermode losses. In this regime the supermode beat length becomes much smaller than the supermode decay length, opening the possibility of building a directional coupler that exhibits only a fraction of modal losses along the coupling length. Because of the multimoded nature of hollow PBG Bragg fibers, special care should be taken to avoid accidental modal degeneracies between the mode of operation and higher-order modes at the frequency of interest.

## APPENDIX A

A multipole method has been introduced to solve for the leaky modes of microstructured fibers;<sup>13</sup> it relies on enforcing consistency between local and global expansions of the electromagnetic fields in the interstitial region between cylinders (cladding region in our case). In what follows, we adapt the original method to treat coupled Bragg fibers. The transverse wave vector is  $k^t = [(kn_{\text{clad}})^2 - \beta^2]^{1/2}$ , and  $(r_j, \theta_j)$  are the local coordinates associated with the center of fiber  $j$  ( $j = 1, 2$ ). In the vicinity of Bragg fiber  $j$ , local expansion of electromagnetic fields is valid in an annulus extending from the surface of fiber  $j$  to the surface of the other fiber and can be expanded in series:

$$\begin{pmatrix} E_z \\ H_z \end{pmatrix} = \sum_m \left[ \begin{pmatrix} A_m^j \\ C_m^j \end{pmatrix} J_m(kr_j) + \begin{pmatrix} B_m^j \\ D_m^j \end{pmatrix} H_m^+(kr_j) \right] \exp(im\theta_j). \quad (\text{A1})$$

An alternative expansion that is due to Wijngarrd that is valid everywhere in the cladding region is

$$\begin{pmatrix} E_z \\ H_z \end{pmatrix} = \sum_{j=1}^2 \sum_m \begin{pmatrix} B_m^j \\ D_m^j \end{pmatrix} H_m^+(kr_j) \exp(im\theta_j). \quad (\text{A2})$$

One enforces the consistency between the two presentations by using Graf's addition theorem for Bessel functions. If symmetry is present, one can reduce the number of independent variables: for example, in our case symmetry of supermode<sup>+</sup> forces  $A_0^j = B_0^j = 0$ ,  $(A, B, C, D)_m^2 = (-1)^m (A, B, C, D)_m^1$ ,  $(A, B)_m^j = (-1)^{m+1} (A, B)_{-m}^j$ , and  $(C, D)_m^j = (-1)^m (C, D)_{-m}^j$ , and supermode<sup>-</sup> forces  $A_0^j = B_0^j = 0$ ,  $(A, B, C, D)_m^2 = (-1)^{m+1} (A, B, C, D)_m^1$ ,  $(A, B)_m^j = (-1)^{m+1} (A, B)_{-m}^j$ , and  $(C, D)_m^j = (-1)^m (C, D)_{-m}^j$ .

Finally, pairs of coefficients  $(A_m^j, C_m^j)$  and  $(B_m^j, D_m^j)$  are related to each other by the boundary conditions of continuity of tangential fields across the boundaries of Bragg mirrors. In particular, in the core of fiber  $j$ , local expansion (1) contains only  $J_m(kr_j)$  terms. We denote the corresponding expansion coefficients of the fields in the core of fiber  $j$   $(A_{o_m}^j, C_{o_m}^j)$ . In what follows, the expansion coefficients of the fields in the Bragg fiber cladding  $(A_m^j, C_m^j)$  and  $(B_m^j, D_m^j)$  are related to the expansion coefficients in the core  $(A_{o_m}^j, C_{o_m}^j)$  by  $(2 \times 2)$  transfer matrices<sup>15</sup>  $M_m^{AC}(\beta)$  and  $M_m^{BD}(\beta)$ , such that  $(A_m^j, C_m^j) = (A_{o_m}^j, C_{o_m}^j) M_m^{AC}$  and  $(B_m^j, D_m^j) = (A_{o_m}^j, C_{o_m}^j) M_m^{BD}$ . Thus, reexpressing two pairs of cladding expansion coefficients in terms of a single pair of core expansion coefficients in Eqs. (A1) and (A2), one arrives at a modified multipole method to treat coupled Bragg fibers.

White *et al.*<sup>13</sup> defined a  $(2 \times 2)$  matrix of reflection coefficients  $R_m(\beta) = (M_m^{AC})^{-1} M_m^{BD}$  and then expressed a coefficient pair  $(A_m^j, C_m^j)$  in terms of  $(B_m^j, D_m^j)$  as  $(B_m^j, D_m^j) = (A_m^j, C_m^j) R_m$ , later arriving at a homogeneous system of equations of the form  $(B, D)[I - R(\beta)H(\beta)] = 0$  in terms of  $(B_m^j, D_m^j)$  coefficients. When one is dealing with weakly interacting Bragg fibers, this choice of independent variables is not computationally convenient. The reason is as follows: Let  $\beta_m$  corre-

spond to the propagation constant of a leaky mode of angular momentum  $m$  of a stand-alone Bragg fiber. Then  $(A_m^j, C_m^j) = (A_{o_m}^j, C_{o_m}^j) M_m^{AC}(\beta_m) \equiv 0$  by the definition of a leaky mode as being constructed from outgoing  $H^+$  waves only in the cladding region. For weakly interacting Bragg fibers, propagation constants of supermodes  $\beta^\pm$  are close to the propagation constant of a mode  $\beta_m$  of a stand-alone Bragg fiber. Thus, transfer matrix  $M_m^{AC}(\beta)$  is almost degenerate near the true solutions  $\beta^\pm$ , leading to the divergences in the matrix of reflection coefficients  $R_m(\beta)$  when  $\beta \sim \beta^\pm$ . Computationally, the problem arises when one is trying to find propagation constants of supermodes by solving  $\det[I - R(\beta)H(\beta)] = 0$ . At  $\beta_m$  the determinant will exhibit a pronounced divergence, whereas at  $\beta^\pm$  (closely placed near  $\beta_m$ ) the determinant will go to zero, thus generating large derivatives in the neighborhood of a true solution, causing any gradient-based methods to fail to converge. The choice of  $(A_{o_m}^j, C_{o_m}^j)$  as defined above eliminates this problem by ensuring nondivergent derivatives with respect to the propagation constant about a true solution.

Finally, as was noted in Ref. 13, the multipole method converges rapidly when angular-momentum states  $m \in [-M, M]$  are included, where  $M$  is of the order of the largest argument of the Bessel functions on the boundary of a Bragg mirror,  $M \sim 1.5kR_o$ . We have found that rapid convergence holds only for intermirror separations  $d/R_o \geq 0.1$ . For closely spaced fibers ( $0.01 \leq d/R_o \leq 0.1$ ) the number of angular-momentum states  $M$  that need to be included increases rapidly, and for  $d/R_o \leq 0.01$  convergence becomes problematic because of numerical errors of inclusion of high-order  $m$  states. Thus, analysis of closely spaced fibers becomes problematic with the multipole method. The inability of the multipole method to treat almost-touching fibers on the one hand is related to the slow convergence of Bessel series in Graf's addition theorem when the ratio of the Bessel function argument in local expansion [Eq. (A1)]  $rk_n^t$  to the interfiber separation argument  $(2R_o + d)k_n^t$  becomes as large as  $1/2$  (in general, Graf's theory is not applicable at all when this ratio is larger than 1) and, on the other hand, because of the problem in matching local and global field expansions in the narrow intermirror region, requires large-angular-momentum states.

M. A. Skorobogatiy's e-mail address is maksim.skorobogatiy@polymtl.ca.

## REFERENCES

1. C. M. Smith, N. Venkataraman, M. T. Gallagher, D. Muller, J. A. West, N. F. Borrelli, D. C. Allan, and K. W. Koch, "Low-loss hollow-core silica/air photonic bandgap fibre," *Nature* (London) **424**, 657–659 (2003).
2. B. Temelkuran, S. D. Hart, G. Benoit, J. D. Joannopoulos, and Y. Fink, "Wavelength-scalable hollow optical fibres with large photonic bandgaps for CO<sub>2</sub> laser transmission," *Nature* (London) **420**, 650–653 (2002).
3. M. A. van Eijkelenborg, A. Argyros, G. Barton, I. M. Bassett, M. Fellew, G. Henry, N. A. Issa, M. C. J. Large, S. Manos, W. Padden, L. Poladian, and J. Zagari, "Recent progress in microstructured polymer optical fibre fabrication and characterisation," *Opt. Fiber Technol.* **9**, 199–209 (2003).
4. B. H. Lee, J. B. Eom, J. Kim, D. S. Moon, U.-C. Paek, and

- G.-H. Yang, "Photonic crystal fiber coupler," *Opt. Lett.* **27**, 812–814 (2002).
5. G. Kakarantzas, B. J. Mangan, T. A. Birks, J. C. Knight, and P. St. J. Russell, "Directional coupling in a twin core photonic crystal fiber using heat treatment," in *Conference on Lasers and Electro-Optics*, Vol. 56 of OSA Trends in Optics and Photonics Series (Optical Society of America, Washington, D.C., 2001), pp. 599–600.
  6. M. Kristensen, "Mode-coupling in photonic crystal fibers with multiple cores," in *Conference on Lasers and Electro-optics* (Washington, D.C., 2000).
  7. B. J. Mangan, J. C. Knight, T. A. Birks, P. St. J. Russell, and A. H. Greenaway, "Experimental study of dualcore photonic crystal fibre," *Electron. Lett.* **36**, 1358–1359 (2000).
  8. K. Saitoh, Y. Sato, and M. Koshiba, "Coupling characteristics of dual-core photonic crystal fiber couplers," *Opt. Express* **11**, 3188–3195 (2003), <http://www.opticsexpress.org>.
  9. L. Zhang and C. Yang, "Polarization splitter based on photonic crystal fibers," *Opt. Express* **11**, 1015–1020 (2003), <http://www.opticsexpress.org>.
  10. K. Saitoh and M. Koshiba, "Full-vectorial imaginary-distance beam propagation method based on a finite element scheme: application to photonic crystal fibers," *IEEE J. Quantum Electron.* **38**, 927–933 (2002).
  11. F. Fogli, L. Saccomandi, P. Bassi, G. Bellanca, and S. Trillo, "Full vectorial BPM modeling of indexguiding photonic crystal fibers and couplers," *Opt. Express* **10**, 54–59 (2002), <http://www.opticsexpress.org>.
  12. S. G. Johnson, M. Ibanescu, M. Skorobogatiy, O. Weisberg, T. D. Engeness, M. Soljačić, S. A. Jacobs, J. D. Joannopoulos, and Y. Fink, "Low-loss asymptotically single-mode propagation in large-core OmniGuide fibers," *Opt. Express* **9**, 748–779 (2001), [www.opticsexpress.org](http://www.opticsexpress.org).
  13. T. P. White, B. T. Kuhlmey, R. C. McPhedran, D. Maystre, G. C. Martijn de Sterke, and L. C. Botten, "Multipole method for microstructured optical fibers. I. Formulation," *J. Opt. Soc. Am. B* **19**, 2322–2330 (2002).
  14. R. A. Minasian, K. E. Alameh, and E. H. W. Chan, "Photonics-based interference mitigation filters," *IEEE Trans. Microwave Theory Tech.* **49**, 1894–1899 (2001).
  15. P. Yeh, A. Yariv, and E. Marom, "Theory of Bragg fiber," *J. Opt. Soc. Am.* **68**, 1196–1201 (1978).